Available online at www.sciencedirect.com
ScienceDirect
International Journal of Pharmaceutics 342 (2007) 222–230
INTERNATIONAL JOURNAL OF PHARMACEUTICS
www.elsevier.com/locate/ijpharm

Pharmaceutical Nanotechnology

Fluorescent biodegradable PLGA particles with narrow size distributions: Preparation by means of selective centrifugation

Marie Gaumet, Robert Gurny, Florence Delie *

Department of Pharmaceutics and Biopharmaceutics, School of Pharmaceutical Sciences, University of Geneva, University of Lausanne, 30 Quai E. Ansermet, CH-1211 Geneva 4, Switzerland

Received 2 January 2007; received in revised form 27 April 2007; accepted 1 May 2007
Available online 10 May 2007

Abstract

Size is the most studied parameter in the field of nanoparticle characterization but few studies have been performed on biodegradable particles with well-defined sizes. The aim of this work was to prepare fluorescent biodegradable polymeric particles having well-defined sizes and well-characterized surface properties. Poly(D,L-lactide-*co*-glycolide acid) particles were prepared by the emulsion evaporation process. Filtration and centrifugation were used to produce particle fractions in the narrow size range from polydispersed batches, and the efficiency of separation was compared. Selective centrifugation allowed for the preparation of five classes of particles having narrow size distribution (0.1, 0.3, 0.6, 1 and 2 μm). Particles were characterized in terms of size distribution, surface morphology, charge, residual surfactant and hydrophilicity. The results showed similar surface properties for all the batches. 3,3′-Dioctadecyloxacarbo-cyanine perchlorate has been successfully incorporated as a fluorescent dye and its ability to remain associated with the particles during cell culture experiments has been proven. Such particles may be used as an adequate tool for studying cellular uptake.

Keywords: Biodegradable particles; Size distribution; Centrifugation; Fluorescence; Biodegradable; Filtration

1. Introduction

Among the advantages of nanoparticles used as drug delivery systems, their ability to cross physiological epithelial barriers is one of the most important. The influence of physico-chemical properties of nanoparticles on their trans-membranal passage has been often studied by means of latex particles, but rarely with biodegradable polymer incorporating fluorescent dye. To correlate the parameters of nanoparticles with their interaction with biological barriers, it is necessary to have all the properties of the particles under control. Data regarding the exact contribution of the physico-chemical properties of biodegradable polymeric particles for their interaction with biological barriers, such as the gastrointestinal tract, remain to be completely elucidated (Delie, 1998). Up to now, most of the studies on particle uptake have been investigated *in vitro* with polystyrene; however, this polymer is not suitable for controlled release due to its non-biodegradability. The characterization of the physico-chemical properties of biodegradable particles is mandatory for the optimum interpretation of cell culture results in terms of size influence (Maassen et al., 1993). Particle size, the more readily accessible parameter, has been shown to be crucial regarding interaction with cells. Several studies have aimed to correlate cellular uptake with particle size, but comparison of the data often showed ambiguity. For instance, the upper size limit to pass through the intestinal barrier remains unclear, ranging from 700 nm (Durrer et al., 1994) to 10 μm (Jani et al., 1990). Moreover, recent studies present great divergences regarding the level of nanoparticle uptake: Win and Feng have shown an uptake by intestinal cells close to 40% for nanoparticles measuring 261.6 nm (Win and Feng, 2005), whereas Dong and Feng have found only 15% for nanoparticles measuring 304.3 nm (Dong and Feng, 2005). Although they were using the same polymer and same experimental conditions with cells, this discrepancy may be due to different size distribution or surface hydrophilicities, which were not characterized.

The preparation and characterization of well-defined sizes of biodegradable particles remain a challenge. The first objective of this work was to prepare fluorescently labelled biodegradable polymeric particles with well-defined sizes and a narrow size

* Corresponding author. Tel.: +41 22 379 65 73; fax: +41 22 379 65 67.
E-mail address: Florence.delie@pharm.unige.ch (F. Delie).

0378-5173/$ – see front matter © 2007 Elsevier B.V. All rights reserved.
doi:10.1016/j.ijpharm.2007.05.001

distribution. Five sizes were targeted (100 nm, 300 nm, 600 nm, 1 μm and 2 μm) in order to cover the most relevant range for future *in vivo* experiments in the field of drug delivery. As the common preparation methods of poly(D,L-lactide-*co*-glycolide) acid (PLGA) nanoparticles are known to give polydispersed and broadly distributed samples, it appears necessary to separate the different populations obtained.

Among techniques easy to handle, two approaches can be considered to isolate a size population from a polydispersed batch, filtration or centrifugation. Filtration method was compared to centrifugation in terms of separation efficiency and yield.

Further, accurate surface property characterization of the batches was performed in terms of morphology, surface charge and hydrophilicity as well as the determination of residual amount of surfactant.

The third objective was to assess whether the fluorescent dye loaded into particles would not leak out of the particles during *in vitro* experiments.

2. Materials and methods

2.1. Materials

The particles were produced using a polyester, poly(D,L-lactide-*co*-glycolide) acid (PLGA, Resomer® RG502, MW 12,000 Da), purchased from Boehringer-Ingelheim (Ingelheim, Germany). Polyvinylalcohol (PVAL, Mowiol® 4–88, MW 31,000 Da) was obtained from Clariant GmbH (Franckfurt, Germany) and used as a surfactant. The fluorescent dye 3,3′-dioctadecyloxacarbo-cyanine perchlorate (DiO, MW 882) was purchased from Molecular Probes (Leiden, The Netherlands). Rose Bengal was obtained from Sigma Co. (St. Louis, MO, USA). Caco-2 cells were a gift from the Department of Genetics and Microbiology of the Centre Médico-Universitaire (University of Geneva, Switzerland). Hank's balanced salt solution (HBSS), DMEM medium, non-essential amino acids and penicillin–streptomycin solution were purchased from Gibco (Invitrogen™ Life Technologies AG, Basel, Switzerland). Fetal calf serum (FCS) was received from Brunschwig (Basel, Switzerland). The 24-well plates were obtained from Costar® (Corning Inc., New York, NY, USA).

2.2. Methods

2.2.1. Particle preparation

Nanoparticles and microparticles were obtained by the emulsion-evaporation (EE) process. The fluorescent dye, DiO, was encapsulated into particles after solubilization in the organic phase. Briefly, 1 ml of organic phase containing 10% (w/v) of PLGA and 0.01% (w/v) of DiO in methylene chloride was poured into an aqueous solution of PVAL (2 ml for nanoparticles and 25 ml for microparticles) to obtain an oil-in-water emulsion. The PVAL concentration varied from 1% to 5% (w/v) depending on the size range desired. The emulsification process was made in an ice bath by sonication for 30 s using a 3 mm microtip probe sonicator set at 40 W of energy output with the help of a sonifier S-450D® (Branson Ultrasonic S.A, Geneva, Switzerland) for nanoparticle preparation. The emulsion was poured dropwise into 50 ml of water and stirred for 1 h under refrigerated conditions and then for 2 h at room temperature to allow solvent evaporation. For microparticle preparation, the emulsification was done by ultra-homogenization with a stirring rate of 20,500 rpm during 10 min in an ice bath with an ultra-homogenizer IKA®-Labortechnik Ultra-turrax T25 (Janke and Kunkel, Staufen, Germany). The emulsion was left for 12 h at room temperature under magnetic stirring to allow solvent evaporation. The particle suspensions were diluted in water for filtration experiments or collected by centrifugation (Avanti® 30 Centrifuge, Beckman Coulter Inc., Fullerton, CA, USA). The yield of particles has been calculated by the ratio between the mass of particles obtained for each batch and the mass of polymer used for the preparation of the initial batch.

2.2.2. Size separation

2.2.2.1. Filtration. Three filtration systems were evaluated to separate and collect the different particle populations. Steriflip® filtration unit (Millipore Corp., Billerica, CA, USA) and Ultrafree® filtration unit (Millipore Corp., Billerica, CA, USA) were provided with a polyvinylidene difluoride (PVDF) membrane with a cut-off 0.22 μm. The separation mechanism of Steriflip® is facilitated by air vacuum. In case of Ultrafree®, it was facilitated by centrifugation performed at 5,000 for 15 min. The concentration of the nanoparticle suspension was set at 1.2 mg/ml. Micro-Kros® module (Spectrum Laboratories Inc., Rancho Dominguez, CA, USA) is similar to tangential filtration and designed for diafiltration of biological entities (e.g. proteins, viruses, etc.). Tangential flow filtration is initiated by applying pressure to a retentive syringe containing the fluid. The fluid flows through the lumen of fibers, from the full syringe downstream to the empty retentate syringe. The fibers are made of polyethersulfone (PES), delimiting a 0.5 μm cut-off.

2.2.2.2. Selective centrifugation. Optimization of each centrifugation step was needed to collect a given size population in the pellet or in the supernatant. Centrifugations were performed with the Avanti® 30 Centrifuge (Beckman Coulter Inc., Fullerton, CA, USA), by adapting the residual centrifuge force (RCF) and the centrifugation time for each particle batch. Furthermore, the number of centrifugation steps has to be sufficient to eliminate a large amount of PVAL to have comparable amount of residual surfactant in resulting batches.

2.2.3. Size characterization

2.2.3.1. Light scattering. During the centrifugation optimization steps, the mean size, the size distribution and polydispersity index (PI) were obtained by dynamic light scattering (DLS) using a compact goniometer ALV/CGS®-5 (ALV-GmbH, Langen, Germany), at room temperature in milli-Q® water at adequate scattering angle for a given size distribution studied. For routine measurements, size parameters were determined with the Zetasizer® 3000HS (Malvern Instruments, Worcesterhire, UK) at 90° scattering angle and recorded for a time determined by the zetasizer program in the automatic mode.

2.2.3.2. Laser light diffraction. Alternative to the DLS, size measurements for microparticles were obtained by laser light diffraction (LLD) with a Mastersizer® S (Malvern Instruments, Worcesterhire, UK). These measurements were performed using the small-volume sample dispersion unit.

2.2.3.3. Scanning electron microscopy. Particles were diluted in distilled water, dropped onto stubs, air dried, covered by a 15–20 nm layer of gold and then examined by scanning electron microscopy (SEM), using a JSM-6300® (JEOL, Tokyo, Japan). Mean particle size was analyzed from SEM pictures using the software ImageJ® (U. S. National Institutes of Health, Bethesda, MA, USA) on at least 200 particles to compare with the results obtained by DLS or LLD.

2.2.4. Surface characterization

2.2.4.1. Morphology. Surface morphology observations were performed by SEM on a Philips® XL-30 (Philips, Lancashire, UK). The particles were diluted in distilled water, dropped onto stubs, air dried, and covered by a thin platinum layer (5–10 nm) before observation.

2.2.4.2. Charge. Zeta potential, directly related to the surface charge density, was determined by electrophoretic mobility on particle suspensions in a 1 mM NaCl solution, at room temperature using the aqueous flow cell in the automatic mode of the Zetasizer® 3000HS (Malvern Instruments, Worcesterhire, UK).

2.2.4.3. Hydrophilicity. Surface hydrophilicity was evaluated by measuring the adsorption of the hydrophilic dye rose bengal (RB) onto the particles. RB will partition between the aqueous phase and the surface of the particles (Müller, 1991). Briefly, a set amount of particles was incubated for 3 h under vortexing at room temperature with RB aqueous solutions at different concentrations (from 2 to 75 μg/ml). After centrifugation, RB concentration was determined in the supernatant by spectrometry at 548 nm (Safire®, Tecan, Salzburg, Austria). The amount of RB adsorbed on the surface of the particles was then calculated by difference. The parameter H (10^{-10} g/m^2) representing the amount of RB bound per surface of particles was calculated with the following equation:

$$H = \frac{0.01Ndr}{3}$$

where N is the maximum amount of RB bound per mass of particles (μg/mg), d is the particle density (1.5 g/cm^3) and r is the particle radius (nm).

2.2.4.4. Residual surfactant determination. The percentage of residual surfactant was measured by a colorimetric assay based on the formation of a complex iodine-PVAL in the presence of boric acid at 635 nm (Sakurada, 1985).

2.2.5. DiO incorporation

The amount of DiO incorporated was determined by spectrofluorimetry (fluorescence spectra in methylene chloride: $\lambda_{ex}/\lambda_{em}$ = 489 nm/506 nm) after particle solubilization in methylene chloride (1 mg/ml).

2.2.6. Cell incubation experiments

The Caco-2 cells were cultivated according to a standard protocol (Pietzonka et al., 2002). Briefly, the cells were seeded in 24-well plates (20,000 cells/well) and grown in an atmosphere of 5% CO_2 using DMEM culture medium supplemented with 10% FCS, 1% of non-essential amino acids and 1% of penicillin and streptomycin. Cells were grown for 2 weeks before experiments, while the medium was changed every other day. To evaluate the possible release of the marker DiO, Caco-2 cells were incubated with DiO loaded-particles (mean size = 2.29 μm, concentration 2 mg/ml) for 4 h at 37 °C, and then washed with HBSS buffer before fluorescence microscopy observation (Axiovert® 200, Zeiss, Göttingen, Germany).

3. Results

3.1. Particle preparation

Three batches of particles differing in size range were obtained by varying the PVAL concentration and the emulsification process: nanoparticles were produced by sonication whereas microparticles were obtained by ultra-homogenization (Table 1). As expected, high concentration of PVAL (5%, w/v) in the aqueous phase gave smaller particles (approximately 250 nm), whereas larger sizes of 340 nm were prepared with 1% (w/w) PVAL. The microparticles (approximately 2000 nm) were obtained by ultra-homogenization and with a concentration of 2% (w/v) of the surfactant. SEM pictures showed broad size distribution (Fig. 1). The SEM observations revealed nanoparticles of <400 nm for batch #1, while for batch #2 the size range was from 100 to 700 nm, showing a larger dispersity than expected with the distribution graphs generated from DLS measurements (Fig. 2). The microparticles had a polydispersed population, ranging from 800 nm to 2.5 μm (batch #3).

Table 1
Characterization of nano- and microparticles

	Batch #		
	1	2	3
PVAL (w/v)	5%	1%	2%
Emulsification mode	Sonication	Sonication	Ultra-homogenization
Mean size[a] (nm)	253 ± 16	340 ± 19	1887 ± 290
Polydispersity	0.10 ± 0.01[b]	0.12 ± 0.02[b]	1.3 ± 0.0[c]
Size observed by SEM (nm), n = 200 ± S.D.	142 ± 51	244 ± 139	1269 ± 537
Yield% (w/w), n = 3 ± S.D.	74 ± 7	85 ± 4	93 ± 8

[a] Obtained by DLS (Zetasizer® 3000HS) for nanoparticles and by LLD (Mastersizer® S) for microparticles, n = 3 ± S.D.
[b] Polydispersity index, scale from 0 to 1, n = 3 ± S.D.
[c] Span, n = 3 ± S.D.

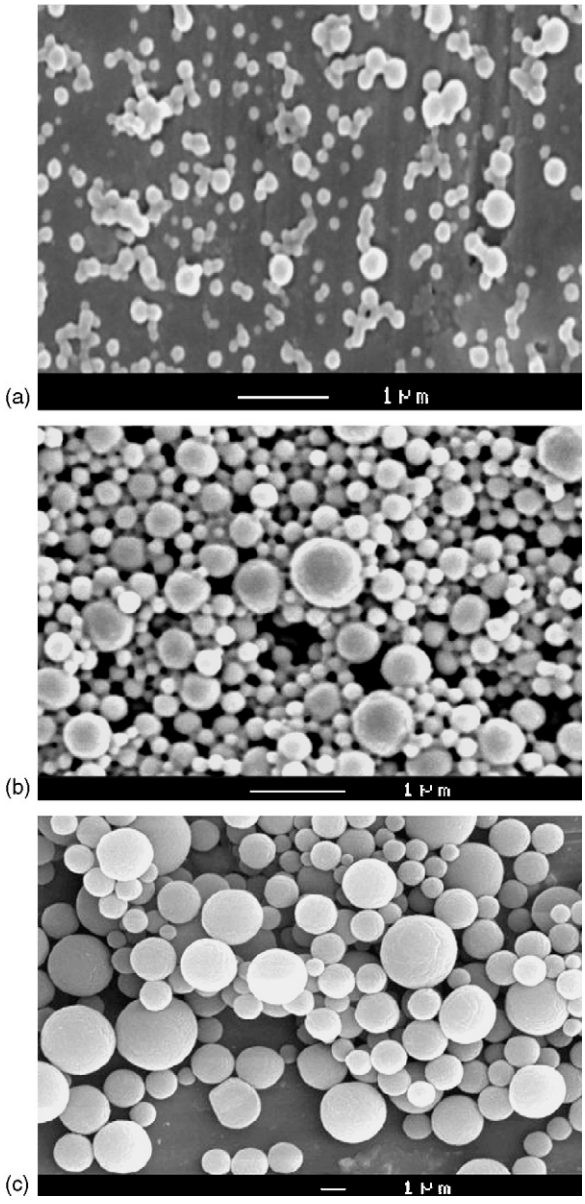

Fig. 1. Scanning electron micrograph of the three initial batches. (a) 253 nm (PI = 0.12), magnification: 20,000×, (b) 340 nm (PI = 0.10), magnification: 20,000× and (c) 1887 nm (span = 1.3), magnification: 5,000.

3.2. Particle separation

Size separation techniques were evaluated to separate the populations present in the three batches to obtain final fractions with a narrow size distribution.

3.2.1. Filtration

The results obtained with the Steriflip®, Ultrafree®, Micro-Kros® systems are summarized in Table 2. The first two filtration systems allowed to obtain monodispersed particles, with low PI: 0.06 and 0.05 for Steriflip® and Ultrafree®, respectively. The yield, expressed by mass of particles collected in the filtrate per mass of particles in the initial suspension, was respectively of 20% for Micro-Kros® and less than 5% for other filtration methods, because of the rapid caking phenomenon. Furthermore, SEM observations of the retentate have shown that many small particles did not cross the filter. None of these techniques was considered satisfactory.

3.2.2. Selective centrifugation

Centrifugation steps were applied on the initial batches to separate different size populations and to obtain final batches with a narrow size distribution. The centrifugation parameters and the particle sizes are listed in Table 3. Based on the principle of RCF and by varying the centrifugation time (at least 15 min), the centrifugation has become selective, leading to the separation of five batches of particles. A minimum of four centrifugation steps were applied on each batch to obtain the desired sizes and also to partially eliminate the surfactant.

Particle size of each batch was accurately measured by DLS (goniometer ALV/CGS®-5), by adapting the scattered angle. Three nanoparticle classes were obtained with sizes of approximately 100, 300 and 600 nm, and two classes of microparticles having sizes near 1 and 2 μm. The size distribution graphs of the five batches can be compared to those obtained for the three initial batches (Fig. 2). Yields are close to 15% for the 100, 300 and 1000 nm particles, and close to 35% and 25% for the 600 and 2000 nm particles, respectively. The low PIs (between 0.06 and 0.08) were confirmed by electron microscopy observations (Fig. 3) with a size range ±20% for each class. The five batches obtained after selective centrifugation were kept in suspension and stored at 4 °C and characterized shortly after in terms of surface properties.

Table 2
Filtration tests performed on nanoparticle batches: sizes before and after filtration

Filtration unit	Steriflip®	Ultrafree®	Micro-Kros®
Membrane cut-off (μm)	0.22	0.22	0.5
Filtration surface (cm^2)	6.7	0.8	8.0
Mean size before filtration[a] (PI[b])	287 ± 5 nm (0.16 ± 0.04)	287 ± 5 nm (0.16 ± 0.04)	463 ± 16 nm (0.16 ± 0.04)
Filtrate mean size[a] (PI[b])	239 ± 1 nm (0.06 ± 0.02)	210 ± 2 nm (0.05 ± 0.02)	216 ± 8 nm (0.07 ± 0.03)
SEM observations of the retentate[c]	Many particles <200 nm in the retentate	Many particles <200 nm in the retentate	Many particles <500 nm in the retentate
Limitations	Caking; membrane breakdown	Caking; volume filtrated (only 2 ml)	Time consuming

[a] Obtained by DLS (Zetasizer® 3000HS), $n = 3 \pm$ S.D.
[b] Polydispersity index, scale from 0 to 1, $n = 3 \pm$ S.D.
[c] Pictures not shown.

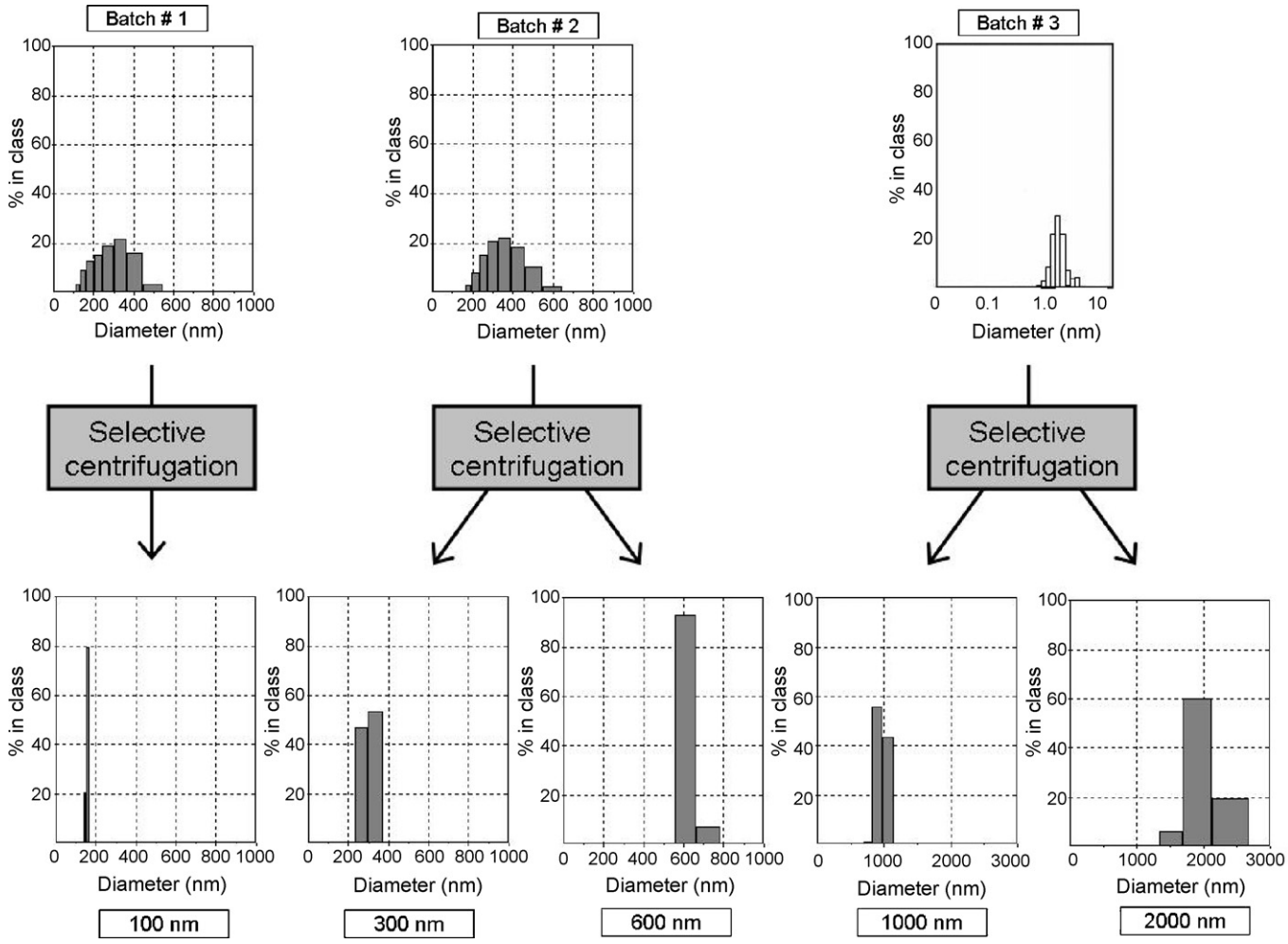

Fig. 2. Size distribution histograms of the batches before and after selective centrifugation. Each graph represents one measurement performed by DLS (Zetasizer® 3000HS) except for the batch #3 measured by LLD (Mastersizer® S).

3.3. Surface morphology

Particle surface analysis at high magnification (Fig. 4) showed an irregular surface not seen at lower magnification (Fig. 3). Even if the particles appeared spherical with a smooth surface at standard magnification (10,000×), their surface was revealed to be irregular at very high magnification (75,000×). Indeed, particle surface seemed to be made of aggregates measuring approximately 20–60 nm in diameter.

Table 3
Particle characterization after selective centrifugation

Initial batches	RCF[a] (g)	Final batches				
Size (nm)		DLS			SEM ($n = 200 \pm$ S.D.)	Yield%[b] (w/w)
		Size[c] (nm)	PI	Scattering angle (°)		
253 ± 16	30,000	166 ± 10	0.08 ± 0.01	125	99 ± 10	11 ± 1
340	4,000	301 ± 9	0.06 ± 0.02	110	229 ± 40	16 ± 2
± 19	275	623 ± 36	0.07 ± 0.03	70	514 ± 90	35 ± 2
1887	167	1124 ± 91	0.07 ± 0.02	115	716 ± 130	15 ± 2
± 290	54	2244 ± 125	0.08 ± 0.03	110	1943 ± 350	26 ± 1

DLS measurements were done in triplicate on a goniometer ALV/CGS®-5 and PI is the polydispersity index (scale from 0 to 1).
[a] Residual centrifuge force.
[b] $n = 3 \pm$ S.D.
[c] Hydrodynamic mean diameter.

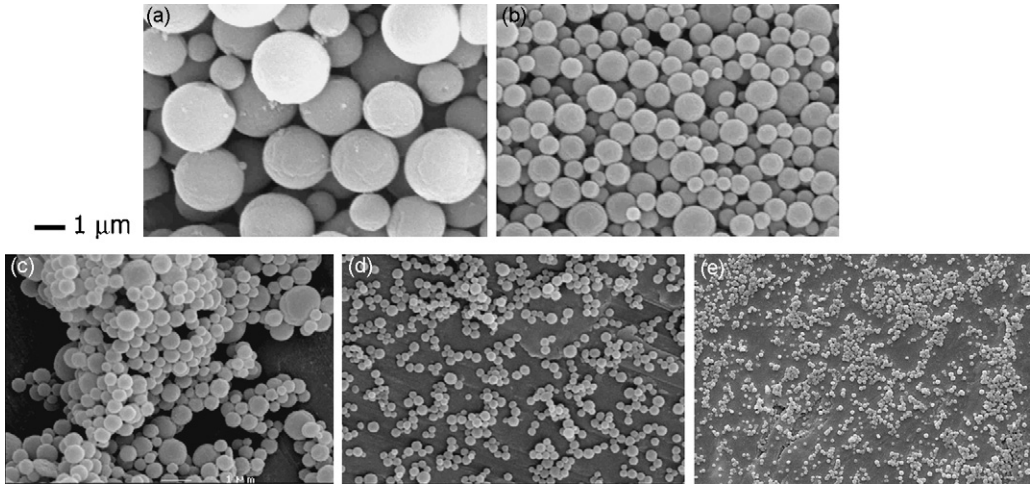

Fig. 3. Scanning electron micrograph of the batches obtained after selective centrifugation steps. Mean size: 1943 nm (a), 716 nm (b), 514 nm (c), 229 nm (d) and 99 nm (e) were measured from the SEM pictures with ImageJ®. The five batches are presented at the same magnification (10,000×).

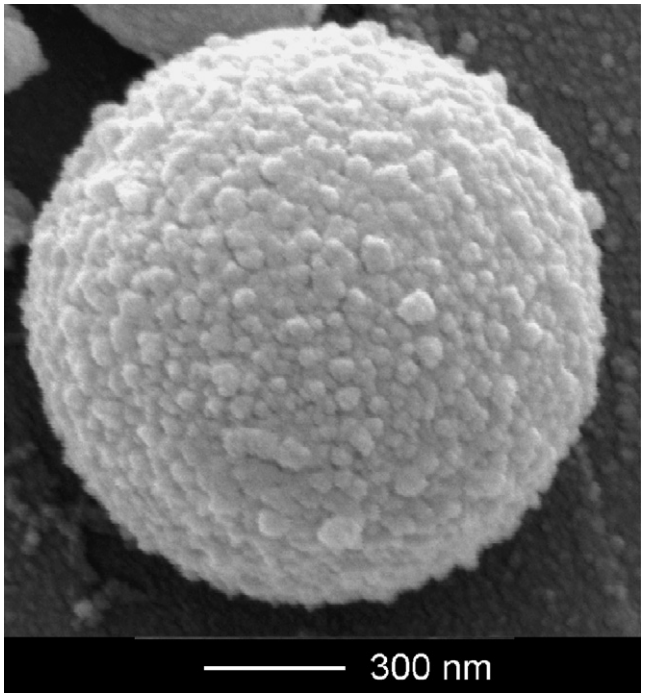

Fig. 4. Scanning electron micrograph of the particle surfaces. Irregular structures can be observed at high magnification (Philips® XL-30, magnification: 75,000×).

3.4. Surface characterization

Surface characterization data are summarized in Table 4. All the particles were negatively charged around −12 mV at pH 7. The zeta potential values were compared for the five batches by analysing variances (ANOVA) with one factor. All values were assessed as statistically equal by the ANOVA test, with a confidence level of 99%. The maximum amount of RB adsorbed onto the particle surface remains comparable at approximately 5×10^{-10} g/m^2 between the five batches. The hydrophilicity data were also assessed as statistically equal by the ANOVA test, with a confidence level of 99%. Finally, the residual amount of PVAL is in the range of 1–3% (w/w), independent of the particle size.

3.5. DiO loading and stability in the presence of cells

For all the batches, an average of $(9.3 \pm 0.4) \times 10^{-4}$% (mass of DiO per mass of PLGA) was encapsulated, which represents encapsulation rates higher than 90%.

The experiments with Caco-2 cells did not show any release of the dye into the medium nor in any cell compartments (Fig. 5).

4. Discussion

Many studies have been carried out on the in vivo fate of colloidal polymeric particles as therapeutic carriers but only few of them deal with the impact of well-defined biodegradable parti-

Table 4
Surface properties of the isolated particles

Batch #	Mean size (nm)	Zeta potential[a] (mV)	Hydrophilicity[a] (10^{-10} g/m^2)	Residual PVAL[a] (%, w/w)
100	168	−10.4 ± 2.8	5.8 ± 1.0	3.4 ± 0.8
300	301	−11.1 ± 1.3	4.7 ± 0.5	2.3 ± 0.8
600	623	−12.7 ± 0.3	5.1 ± 0.5	1.4 ± 0.5
1000	1124	−12.1 ± 0.1	5.7 ± 1.2	1.3 ± 0.4
2000	2244	−11.9 ± 0.7	6.5 ± 2.0	0.7 ± 0.2

[a] $n = 3 \pm$ S.D.

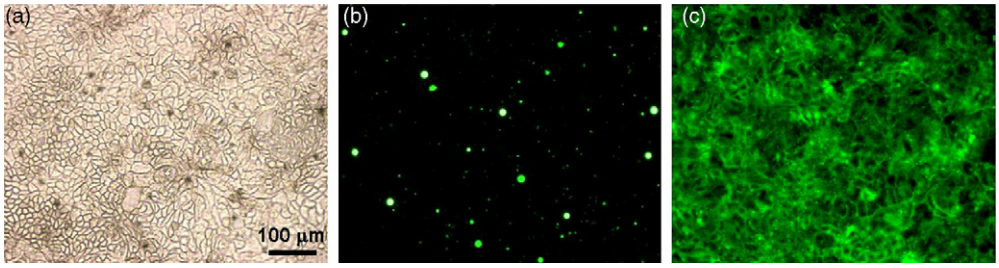

Fig. 5. Fluorescence microscopy images of Caco-2 cells after 2 h incubation at 37 °C with particles loaded in DiO (green fluorescent signal). (a) Transmission, (b) fluorescence and (c) fluorescence: control with the free DiO. Mean size of the particles: 2.29 μm, concentration incubated: 2 mg/ml. No labelling of cell membranes or compartments can be noticed indicating that no release of the DiO has occurred.

cles in terms of size distribution and surface properties (charge and hydrophilicity). In this context, only establishment of processes to obtain particle batches with narrow size distribution and well-characterized surface properties will allow the accurate determination of the parameters directly involved in their relationship with biological barriers. Understanding the parameters involved in this interaction is crucial to design efficient nanoparticles as drug delivery systems.

In this study, we aimed to prepare PLGA nanoparticles of five sizes from 100 to 2000 nm (100, 300, 600, 1000 and 2000 nm) which correspond to the most used in the studies performed *in vivo* with polystyrene particles. Therefore, five batches with low PI were prepared and characterized. Their narrow size distributions were demonstrated by LS and confirmed by SEM images (Table 3; Figs. 2 and 3). Many preparation methods are available to manufacture nanoparticles. In a preliminary set of experiments (data not shown), salting-out process (Ibrahim et al., 1992) and nanoprecipitation technique (Fessi et al., 1989) were evaluated to produce the targeted sizes, but seemed less suitable for our application. Indeed, salting-out method uses very high concentration of PVAL and salts, particularly to generate small sizes, which involves tedious purification steps and difficulty of working on a small scale (Sahoo et al., 2002). Nanoprecipitation technique offers only few process parameters; therefore, it is difficult to vary the nanoparticle size in the range we wanted to explore. With EE, obtaining different particle sizes was achieved by varying homogenization parameters and concentration of PVAL while keeping low amount of this polymer. An increase in surfactant concentration resulted in a decrease in particle size (Julienne et al., 1992).

Applying this technique, preliminary studies showed that it was very difficult to reach high size homogeneity with particles made of PLGA. Polydispersed batches were prepared first (Fig. 1), then different fractions of size were separated. This approach allowed to prepare different sizes of particles from one single batch, limiting the risk of modifying the surface properties by changing manufacturing parameters. Indeed, to study the size effect on the particle–cell interaction, particles need to possess identical properties, such as surface hydrophilicity and charge (Müller et al., 1997).

Information about the size distribution of the batches obtained by the EE method was crucial (Table 1). The standard deviation (S.D.) mentioned in Table 1 is a statistical calculation that indicates the distribution of the size around the mean. Typically, size measurement is repeated several times on the same sample. The results are gathered for each run and pooled together as a mean size and standard deviation. The S.D. given by LS does not represent the variation on the whole particle population but the error made on three measures and not the distribution of the particle population. Data obtained by DLS for batches #1 and #2 were satisfactory with a low PI (0.10 for the 253 nm particles and 0.12 for the 340 nm particles). SEM pictures showed, however, heterogeneous size distributions (Fig. 1). The detailed analysis for the batch #2 revealed particles measuring 300 nm but also many particles under 200 nm and over 500 nm (Fig. 1b). Ideally, if the mean diameter is 340 nm, the majority of the population should be between 300 and 400 nm. These results illustrate that the polydispersity index measured routinely by light scattering may be far from the reality shown by microscopy images: a nanoparticle batch appears often more polydispersed in microscopy than how it is indicated by its PI value (Shakweh et al., 2005). Furthermore, the mean size appears overestimated by DLS because the hydrodynamic volume is measured and larger particles show greater contributions to the scattering whereas it is underestimated by SEM because dried particles are observed. The data summarized in Table 2 illustrate this point: the mean size of the nanoparticles collected in the filtrate is higher than the membrane cut-off. The value of 210 nm for the particles filtrated with Ultrafree® is over-evaluated by DLS measurements. The presence of aggregates can also explain this result; however, this is not likely when considering the low PI of 0.05 and SEM observations (data not shown).

In summary, the first particle preparation step gave polydispersed batches from which batches having a monomodal and narrow size distribution can be collected by adequate separation. The comparison of the different filtration systems showed that none of them led to satisfactory results. Indeed, with all the systems tested, clogging and loss of matter occurred. Practically, only low amounts of particles can be filtrated with Steriflip® and Ultrafree® because of a rapid caking phenomenon. Even if collection of two fractions has been possible, the system Micro-Kros® appears unsuitable for nanoparticle separation because many particles under the membrane cut-off remain in the retentate. Konan et al. reported the use of filtration for sterilization purposes without clogging or loss of matter (Konan et al., 2002) but the initial batches were highly uniform in size with a mean size below the filtration cut-off. Another study reports the fractionation of PLGA nanoparticles having a bimodal size

distribution (100 and 400 nm) by passing through a PVDF membrane with a cut-off of 100 nm (Prabha et al., 2002). However, the conditions applied (under nitrogen pressure and with a flow rate of 0.06 ml/min) are specific to handle and the yield obtained (less than 5%) is very low. Our study confirms the difficulty of obtaining different sizes from the same initial batch by simple filtration systems, without the caking of nanoparticles and with a sufficient yield.

Selective centrifugation method appeared to be more adapted to nanoparticle size separation. Usually, repeated centrifugation steps are required to collect particles in suspension and to remove the surfactant. In our case, this process presents the advantage of allowing the separation from heterogeneous batches. To ensure reproducibility, parameters such as concentration and volume of the nanoparticle suspension have to be under control. So, the objective of obtaining five particle batches differing in size and with low PI was achieved (Table 3 and Fig. 2). Furthermore, the SEM pictures and their analysis with ImageJ® confirmed their homogeneity in size (Fig. 3).

Our objective was to achieve a complete characterization of the particles; SEM observations were performed at high magnification to check the surface of the particles. A smooth surface is usually described in the literature for this kind of particles (Shakweh et al., 2005; Win and Feng, 2005). Nanoparticle surface was not smooth but appeared as made of small structures (Fig. 4), giving an irregular aspect to the particle surface. Several hypotheses can be proposed. First, the presence of residual surfactant could explain these structures. The low percentage of residual PVAL determined by spectrometry (Table 4) does not support this hypothesis; the amount of surfactant seems too low to cover the entire particle surface. Secondly, it might be the image of the polymer chains framework within the nanoparticle. Indeed, a polymeric nanoparticle can be schematized as an aggregate of several polymeric chains but their accurate intrinsic structure remains unclear (Faisant et al., 2002). It might be also related to the onset of the polymer erosion process at the particle surface. Of course, the possibility of an artefact due to the platinum layer used for SEM sample preparation cannot be excluded. Even if the second hypothesis seems the most likely, we cannot reach any conclusion without further investigations. Furthermore, to our knowledge, no other investigation at such a high magnification of similar particles has been carried out.

Surface charge and hydrophilicity data show similar properties for each of the particle batches. Residual surfactant rates are low compared to data from literature regarding particles prepared in comparable conditions (Zambaux et al., 1998; Panyam et al., 2003). This result shows that the preparation method (EE) followed by a separation process (selective centrifugation) yields batches of different size but having the same surface properties. This feature will allow to accurately compare the impact of the size contribution on a biological effect, independent of the surface properties.

Finally, the encapsulation of the DiO as a fluorescent marker and its ability to remain within the particles during incubation with cells (Fig. 5) has been demonstrated. The choice of the dye is crucial to avoid undesired release from the particles during the *in vitro* studies. The dye has to remain associated to the particle matrix to study particle location without artefact due to the diffusion of the marker within the cellular compartments. For instance, a study demonstrated that the leakage of currently used dyes such as Nile red and its diffusion into the lipophilic compartments of the cell strongly affected the quantitative evaluation of particle uptake (Pietzonka et al., 2002). The same problem has been recently observed in our laboratory (Nobs et al., 2006). The low molecular weight of the Nile red and its high affinity for labelling the lipophilic cell compartments could explain its release from the polymeric matrix of the particle. For these reasons, a less common dye such as the DiO has been chosen for this application, which is highly soluble in methylene chloride and has a high fluorescent quantum yield. Its stability as cell membrane marker associated with its low tendency to transfer between intact membranes could prove to be favorable toward its use as a particle dye.

In summary, by setting a well-defined method of preparation, it was possible to obtain fluorescent particles with narrow size distributions from batches manufactured under comparable conditions. It has been demonstrated that zeta potential and hydrophilicity of all the particles are similar and that the amount of residual surfactant is very low. DiO as marker has been successfully encapsulated and remains associated with the particles when in contact with cells; this will help in the further studies of cellular trafficking.

Acknowledgments

The authors are grateful to Nathalie Boulens and Catherine Siegfried (School of Pharmaceutical Sciences, University of Geneva, Switzerland) and Marcel Düggelin (Biocenter, University of Basel, Switzerland) for their technical assistance in the generation of SEM images. The authors also wish to thank Professor Borkovec (Department of Inorganic, Analytical, and Applied Chemistry, University of Geneva, Switzerland) for having placed the compact goniometer ALV/CGS®-5 (ALV-GmbH, Langen, Germany) at their disposal.

References

Delie, F., 1998. Evaluation of nano- and microparticle uptake by the gastrointestinal tract. Adv. Drug Deliv. Rev. 34, 221–233.

Dong, Y., Feng, S.S., 2005. Poly(D,L-lactide-*co*-glycolide)/montmorillonite nanoparticles for oral delivery of anticancer drugs. Biomaterials 26, 6068–6076.

Durrer, C., Irache, J., Duchêne, D., Ponchel, G., 1994. Study of the interactions between nanoparticles and intestinal mucosa. Prog. Colloid Polym. Sci. 97, 275–280.

Faisant, N., Siepmann, J., Benoit, J.P., 2002. PLGA-based microparticles: elucidation of mechanisms and a new, simple mathematical model quantifying drug release. Eur. J. Pharm. Sci. 15, 355–366.

Fessi, H., Puisieux, F., Devissaguet, J.P., Ammoury, N., Benita, S., 1989. Nanocapsule formation by interfacial polymer deposition following solvent displacement. Int. J. Pharm. 55, R1–R4.

Ibrahim, H., Bindschaedler, C., Doelker, E., Buri, P., Gurny, R., 1992. Aqueous nanodispersions prepared by a salting-out process. Int. J. Pharm. 87, 239–246.

Jani, P., Halbert, G.W., Langridge, J., Florence, A.T., 1990. Nanoparticle uptake by the rat gastrointestinal mucosa: quantitation and particle size dependency. J. Pharm. Pharmacol. 42, 821–826.

Julienne, M.C., Alonso, M.J., Gomez Amoza, J.L., Benoit, J.P., 1992. Preparation of poly(D,L-lactide/glycolide) nanoparticles of controlled particle size distribution: application of experimental designs. Drug Dev. Ind. Pharm. 18, 1063–1077.

Konan, Y.N., Gurny, R., Allemann, E., 2002. Preparation and characterization of sterile and freeze-dried sub-200 nm nanoparticles. Int. J. Pharm. 233, 239–252.

Maassen, S., Fattal, E., Müller, R.H., Couvreur, P., 1993. Cell cultures for the assessment of toxicity and uptake of polymeric particulate drug carriers. S.T.P. Pharma 3, 11–22.

Müller, R.H., 1991. Surface hydrophobicity. In: Müller, R.H. (Ed.), Colloidal carriers for controlled drug delivery targeting. CRC Press, Boca Raton, Florida, pp. 99–109.

Müller, R.H., Ruhl, D., Luck, M., Paulke, B.R., 1997. Influence of fluorescent labelling of polystyrene particles on phagocytic uptake, surface hydrophobicity, and plasma protein adsorption. Pharm. Res. 14, 18–24.

Nobs, L., Buchegger, F., Gurny, R., Allemann, E., 2006. Direct and two step antibody tumor targeting with biodegradable nanoparticles. Bioconjugate Chem. 17, 139–145.

Panyam, J., Sahoo, S.K., Prabha, S., Bargar, T., Labhasetwar, V., 2003. Fluorescence and electron microscopy probes for cellular and tissue uptake of poly(D,L-lactide-*co*-glycolide) nanoparticles. Int. J. Pharm. 262, 1–11.

Pietzonka, P., Rothen-Rutishauser, B., Langguth, P., Wunderli-Allenspach, H., Walter, E., Merkle, H.P., 2002. Transfer of lipophilic markers from PLGA and polystyrene nanoparticles to Caco-2 monolayers mimics particle uptake. Pharm. Res. 19, 595–601.

Prabha, S., Zhou, W.Z., Panyam, J., Labhasetwar, V., 2002. Size-dependency of nanoparticle-mediated gene transfection: studies with fractionated nanoparticles. Int. J. Pharm. 244, 105–115.

Sahoo, S.K., Panyam, J., Prabha, S., Labhasetwar, V., 2002. Residual polyvinyl alcohol associated with poly(D,L-lactide-*co*-glycolide) nanoparticles affects their physical properties and cellular uptake. J. Control. Release 82, 105–114.

Sakurada, I., 1985. Chemical reactions of polyvinyl alcohol. International Fiber Science and Technology Series: Polyvinyl Alcohol Fibers, vol. 6. Marcel Dekker Inc., New York, pp. 137–159.

Shakweh, M., Besnard, M., Nicolas, V., Fattal, E., 2005. Poly(lactide-*co*-glycolide) particles of different physicochemical properties and their uptake by peyer's patches in mice. Eur. J. Pharm. Biopharm. 61, 1–13.

Win, K.Y., Feng, S.S., 2005. Effects of particle size and surface coating on cellular uptake of polymeric nanoparticles for oral delivery of anticancer drugs. Biomaterials 26, 2713–2722.

Zambaux, M.F., Bonneaux, F., Gref, R., Maincent, P., Dellacherie, E., Alonso, M.J., Labrude, P., Vigneron, C., 1998. Influence of experimental parameters on the characteristics of poly(lactic acid) nanoparticles prepared by a double emulsion method. J. Control. Release 50, 31–40.